Molecular Biology of the Cell
Vol. 17, 4270–4281, October 2006

Organization of the Integrin LFA-1 in Nanoclusters Regulates Its Activity[D]

Alessandra Cambi,* Ben Joosten,* Marjolein Koopman,† Frank de Lange,*‡ Inge Beeren,* Ruurd Torensma,* Jack A. Fransen,‡ Maria Garcia-Parajó,†§ Frank N. van Leeuwen,* and Carl G. Figdor*

*Department of Tumor Immunology and ‡Department of Cell Biology and Microscopic Imaging Centre, Nijmegen Centre for Molecular Life Sciences, Radboud University Nijmegen Medical Centre, 6500 HB Nijmegen, The Netherlands; and †Applied Optics Group and Department of Applied Physics and MESA+ Research Institute, University of Twente, 7522 NM Enschede, The Netherlands

Submitted December 2, 2005; Revised June 29, 2006; Accepted July 6, 2006
Monitoring Editor: Martin A. Schwartz

The β2-integrin LFA-1 facilitates extravasation of monocytes (MOs) into the underlying tissues, where MOs can differentiate into dendritic cells (DCs). Although DCs express LFA-1, unlike MOs, they cannot bind to ICAM-1. We hypothesized that an altered integrin organization on the DC plasma membrane might cause this effect and investigated the relationship between membrane organization and function of LFA-1 on MOs and DCs. High-resolution mapping of LFA-1 surface distribution revealed that on MOs LFA-1 function is associated with a distribution in well-defined nanoclusters (100–150-nm diameter). Interestingly, a fraction of these nanoclusters contains primed LFA-1 molecules expressing the specific activation-dependent L16-epitope. Live imaging of MO–T-cell conjugates showed that only these primed nanoclusters are dynamically recruited to the cellular interface forming micrometer-sized assemblies engaged in ligand binding and linked to talin. We conclude that besides affinity regulation, LFA-1 function is controlled by at least three different avidity patterns: random distributed inactive molecules, well-defined ligand-independent proactive nanoclusters, and ligand-triggered micrometer-sized macroclusters.

INTRODUCTION

Integrins are transmembrane α/β heterodimers that regulate cell–cell and cell–extracellular matrix interactions. Lymphocyte function-associated antigen-1 (LFA-1; $\alpha L\beta 2$; CD11a/CD18) is a leukocyte specific integrin that mediates migration across the endothelium and within tissues and formation of immunological synapse (Dustin and Springer, 1989; van Kooyk *et al.*, 1989; Lub *et al.*, 1995; Grakoui *et al.*, 1999; Carman *et al.*, 2003). LFA-1 binds to its major counterreceptor ICAM-1 (Marlin and Springer, 1987) and with lower affinity also to ICAM-2 (Staunton *et al.*, 1989) and -3 (de Fougerolles *et al.*, 1991; de Fougerolles and Springer, 1992).

Two not-mutually-exclusive mechanisms were proposed explaining how integrins such as LFA-1 become activated. First, conformational changes lead to an increased affinity for the ligands (Shimaoka *et al.*, 2003). Evidence comes from mutagenesis studies (Lu *et al.*, 2001a; Lu *et al.*, 2001b) and from the identification of "activation reporter" epitopes (Dransfield and Hogg, 1989; Beals *et al.*, 2001). Indeed, NMR and negative stain electron microscopy (EM) have revealed conformational rearrangement and movement, such as separation of the cytoplasmic tails and extension of the extracellular domains, that lead to a general mechanism of integrin activation (Takagi *et al.*, 2002; Vinogradova *et al.*, 2002). Early studies also showed that a Ca^{2+}-dependent epitope recognized by the monoclonal antibody (mAb) NKI-L16 (Keizer *et al.*, 1988; van Kooyk *et al.*, 1991)—further referred to as L16 epitope—is an activation-reporter epitope resulting from a Ca^{2+}-bound extended conformation of the αL subunit (Xie *et al.*, 2004).

A second mechanism that regulates integrin activation is a dynamic reorganization of LFA-1 receptors into multimolecular assemblies at the cell surface that locally increase the binding valency (avidity; van Kooyk *et al.*, 1999; Katagiri *et al.*, 2003). So far, experimental evidence for the formation of such LFA-1 clusters on activated cells is limited and primarily is based on images of micrometer-sized patches of molecules on the plasma membrane of polarized cells (van Kooyk *et al.*, 1994). Whether the formation of integrin clusters precedes or follows ligand binding remains controversial (Bazzoni and Hemler, 1998; Carman and Springer, 2003). It was shown that on T-lymphocytes recruitment of LFA-1 within specialized membrane lipid microdomains enhances LFA-1 clustering (Krauss and Altevogt, 1999; Marwali *et al.*, 2003), which might have direct implications for LFA-1 as a signaling molecule (Leitinger and Hogg, 2002).

Human monocytes (MOs) use LFA-1 to mediate antibody (Ab)-dependent cytotoxicity, to adhere to endothelial cells and extravasate into the underlying tissue (Martz, 1987;

This article was published online ahead of print in *MBC in Press* (http://www.molbiolcell.org/cgi/doi/10.1091/mbc.E05–12–1098) on July 19, 2006.

[D] The online version of this article contains supplemental material at *MBC Online* (http://www.molbiolcell.org).

§ Present address: Laboratory of NanoBioengineering, Parc Científic de Barcelona (PCB), Josep Samitier 1-5, 08028 Barcelona, Spain, and ICREA-Institució Catalana de Recerca i Estudis Avançats, 08015 Barcelona, Spain.

Address correspondence to: Carl G. Figdor (c.figdor@ncmls.ru.nl).

Abbreviations used: LFA-1, lymphocyte function–associated antigen-1; MO, monocytes; DC, dendritic cell; moDC, monocyte-derived dendritic cell; TEM, transmission electron microscopy.

Springer, 1990). Recently, endothelial cells were shown to form upright microvilli-like projections that are enriched in ICAM-1 molecules (Carman *et al.*, 2003). Transmigrating MOs present regions of increased density of LFA-1 molecules that form linear clusters and colocalize with the ICAM-1–enriched projections (Carman *et al.*, 2003). As precursors of antigen-presenting immature dendritic cells (DCs; Banchereau and Steinman, 1998), MOs can differentiate in DCs upon reverse transmigration over endothelial monolayers (Randolph *et al.*, 1998) or when cultured in vitro in presence of GM-CSF and IL-4 (moDCs; Romani *et al.*, 1996). Although moDCs express LFA-1, unlike MOs, adhesion to ICAM-2 and -3 is completely mediated by the C-type lectin DC-SIGN (CD209; Geijtenbeek *et al.*, 2000a, 2000b).

These observations suggest that the plasma membrane organization of adhesion receptors on MOs and DCs must change dynamically, along with the specific alterations occurring during the development from precursors toward DCs. Our previous studies showed that distribution of DC-SIGN at the cell surface dynamically changed during DC development along with its binding properties (Cambi *et al.*, 2004). This prompted us to investigate and compare the relationship between cell membrane organization and adhesiveness of LFA-1 on MOs and DCs. Here, we demonstrate that LFA-1–mediated binding to ICAM-1 is completely lost during development of moDCs. This coincides with gradual exclusion of LFA-1 from lipid microdomains. We used high-resolution transmission EM (TEM) on whole-mount samples of MOs and DCs to map the cell surface distribution of LFA-1 at submicrometer level. Our findings demonstrate the existence of three levels of avidity for LFA-1: randomly distributed inactive molecules, well-defined ligand-independent nanoclusters, and ligand-triggered micrometer-sized macroclusters.

MATERIALS AND METHODS

Monoclonal Antibodies and Chemicals

The mouse mAbs against αL chain: NKI-L15, NKI-L16, and TS2/4 (kindly provided by E. Martz). Activating KIM185, kindly provided by M. Robinson, Celltech (Slough, United Kingdom), and the blocking NKI-L19 recognize the β2 chain. REK-1 is a mAb anti-ICAM-1. CD46 and CD55 were detected by E4.3 (PharMingen) and 143–30 (CLB, Amsterdam, The Netherlands), respectively. Alexa-conjugated secondary Abs, Alexa-488–conjugated cholera toxin B subunit, and the Alexa-647 labeling kit were from Molecular Probes (Eugene, OR) and Invitrogen; methyl-β-cyclodextrin (MCD) from Sigma (St. Louis, MO); rhodamine-conjugated goat anti-mouse IgG H&L Fab fragment from Abcam (Cambridge, United Kingdom); goat anti-CTxB antibody from Calbiochem (La Jolla, CA); goat anti-mouse-conjugated 10-nm gold from Aurion Biosystems (Vienna, Austria). The rat anti-cytohesin-1 Ab 7H2 was a gift of W. Kolanus (University of Bonn, Germany). The rat anti-RAPL Ab E11.2 was a gift of K. Katagiri (Kyoto University, Japan).

Cells

MOs were obtained from buffy coats of healthy individuals and were purified using Ficoll density centrifugation. Immature DCs were obtained as already reported elsewhere (Romani *et al.*, 1994; Geijtenbeek *et al.*, 2000c). The Jurkat T-cell line was kept in culture in Iscove's medium supplemented with 5% fetal calf serum.

Fluorescent Bead Adhesion Assay

Carboxylate-modified streptavidin-coated TransFluorSpheres (488/645 nm, 1 μm ∅; Molecular Probes) were coated with ICAM-1-Fc, and the bead adhesion assay was performed as described (Geijtenbeek *et al.*, 1999). Briefly, the fluorescent beads were coated with biotinylated goat anti-human Fc antbodies and subsequently with ICAM-1-Fc chimeras. This guarantees the outwards orientation of the ICAM-1 molecules with respect to the bead surface. After each coating step, several thorough washing steps ensure that the excess of unbound molecules is washed away. For the incubation, a ratio of 20 beads per cell was used. The blocking or stimulating Abs were preincubated with the cells before adding the ligand-coated beads. When the lipid raft–disrupting agent MCD was used, the cells were resuspended in serum-free medium containing 20 mM MCD and preincubated for 30 min at 37°C. Adhesion was determined as the percentage of cells that bound fluorescent beads by flow cytometry on an FAC-Scalibur (Becton Dickinson, Oxnard, CA).

Flow Cytometry

For flow cytometry analysis, cells were incubated (30 min, 4°C) in PBS, 0.5% BSA, and 0.01% sodium azide, with different mAbs (5 μg/ml), followed by incubation with FITC-labeled goat anti-mouse IgG antibody (GAM-FITC; Zymed, South San Francisco, CA) for 30 min at 4°C. The relative fluorescence intensity was measured on a FACSCalibur. Isotype-specific controls were included.

Confocal Microscopy

For studies of colocalization with lipid rafts, cells were stained with mAbs and CTxB as already described (Cambi *et al.*, 2004). Isotype-specific controls were always included. Analysis was done with a Bio-Rad MRC1024 Confocal Laser Scanning Microscope (Richmond, CA). Signals were collected sequentially to avoid bleed-through. To prevent loss of NKI-L16 binding in the double- or triple-labeling experiments, cells were not fixed before adding the primary Abs. They were allowed to adhere on FN-coated coverslips and stained with anti-LFA-1 (NKI-L16 or NKI-L15, or TS2/4) and anti-ICAM-1 (10 μg/ml) at 4°C, after prolonged incubation in CLSM buffer to minimize a specific binding. After removing unbound Abs by extensive washing in ice-cold PBS, cells were quickly fixed in 1% PFA, and after a blocking step in CLSM buffer, secondary staining for LFA-1 and ICAM-1 was performed using isotype-specific Alexa-conjugated goat anti-mouse antibodies. Manders coefficient M1 was calculated as already reported (Costes *et al.*, 2004) and reflects the amount of LFA-1 colocalizing with GM1 separately for each cell.

Electron Microscopy Labeling Procedure

For TEM, MOs and DCs were allowed to spread on glass coverslips covered by a thin layer of poly-L-lysine (PLL)-coated Formvar for 1 h at 37°C, washed to remove unbound cells, and immediately fixed with 1% PFA for 15 min. Subsequent Ab and gold labeling was performed as already published (Cambi *et al.*, 2004). When labeling was performed using NKI-L16, no prefixation with 1% PFA was performed to prevent loss of NKI-L16 binding. Therefore, after adhesion on the substrate, cells were washed in ice-cold buffer and incubated on ice with cold NKI-L16. Isotype-specific controls were always included. It should be noted that the effect of temperature changes on NKI-L16 labeling is negligible (Supplementary Figure 2).

Analysis of Gold Particle Distribution Pattern

After gold labeling and fixation, the specimens were dehydrated and transferred from the glass onto copper grids as already published (Cambi *et al.*, 2004). The specimens were observed in a JEOL 1010 transmission electron microscope (Welwyn Garden City, United Kingdom), operating at 60–80 kV. Because MOs and DCs widely spread, the membrane available for gold particle analysis represented up to 60–70% of the whole labeled plasma membrane. For each cell several areas were analyzed at random. The digital images of electron micrographs were processed by custom-written software based on Labview (National Instruments, Austin, TX) as already described (Cambi *et al.*, 2004).

Live Imaging

MOs adhered onto a FN-coated glass Petri dish (30 min, 37°C). After extensive washing in cold PBS, MOs were labeled with NKI-L16 (15 min, 4°C) and subsequently with the rhodamine-conjugated goat anti-mouse IgG H&L Fab fragment (15 min at 4°C). After thorough washing, the Alexa-647–conjugated TS2/4 (or NKI-L15) was added for 15 min at RT. After washing in Imaging medium (RPMI 1640, without phenol red), labeled MOs were put on the microscope setup at 37°C and 5% CO_2 for 10 min before imaging started. Subsequently, unlabeled Jurkat T-cells were added, and the interactions were analyzed with a Zeiss LSM 510 microscope, using a PlanApochromatic 63 × 1.4 oil immersion DIC lens (Carl Zeiss GmbH, Jena, Germany). While recording, the pinhole was completely open. Cells were imaged using Zeiss LSM Image Browser version 3.2 (Carl Zeiss) and processed with Image J version 1.32j software (National Institutes of Health, http://rsb.info.nih.gov/ij).

RESULTS

LFA-1–mediated Binding Is Lost During Development of moDCs

We previously showed that moDCs express high amounts of DC-SIGN and moderate amounts of LFA-1. Both receptors are able to bind to ICAM-2 and -3, additionally LFA-1 binds to ICAM-1. While on MOs LFA-1 mediates adhesion to all ICAMs, on DCs adhesion to ICAM-2 and -3 is completely mediated by DC-SIGN (Geijtenbeek *et al.*, 2000a, 2000b; Cambi *et al.*, 2004). In an attempt to understand this change in LFA-

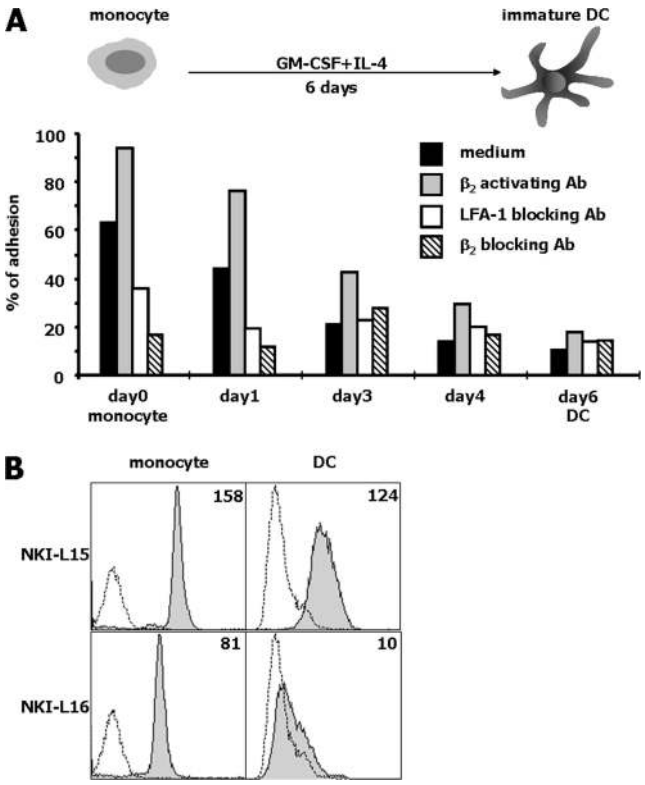

Figure 1. Binding to ICAM-1 and L16 epitope expression decrease during development of moDCs. (A) Adhesion to ICAM-1 during development of moDCs (see drawing) was determined using 1-μm ligand-coated fluorescent beads, prepared as described in *Materials and Methods.* NKI-L15 and NKI-L19 mAbs were used to block LFA-1 and all β2 integrins, respectively. To enhance binding, the anti-β2 activating mAb KIM185 was used. Neither blocking nor activation was observed in presence of isotype controls (unpublished data). One representative experiments out of three is shown. (B) The expression levels of LFA-1 on MOs and DCs were assessed by FACS analysis. □, the isotype control; ▨, the specific staining with anti-LFA-1 mAb. Mean fluorescence intensity is indicated. One representative donor is shown.

1–binding capacity from MOs to DCs, we measured LFA-1–mediated binding to ICAM-1 Fc-coated beads during DC development (Geijtenbeek *et al.,* 1999). MOs and DCs profoundly differ in their capacity to bind ICAM-1–coated fluorescent beads (Figure 1A). More than 60% of MOs spontaneously bound ICAM-1, and this interaction was predominantly β2-integrin mediated, as shown by the effective block in the presence of anti-β2 blocking mAb NKI-L19. The use of anti-αL blocking mAb (NKI-L15) indicated that on MOs, binding to ICAM-1 was predominantly mediated by LFA-1 (40%), whereas the other two β2-integrins MAC-1 and p150.95 mediated the residual binding.

On differentiation of MOs into DCs, spontaneous binding to ICAM-1 gradually decreased. On DCs, residual binding to ICAM-1 was barely detectable and slightly inducible by the anti-β2–activating mAb KIM185. Similarly, other stimuli known to activate LFA-1, such as Mn^{2+}, cytochalasin D, thapsigargin, or PMA, were unable to enhance LFA-1–binding capacity (our unpublished data). Furthermore, no LFA-1–mediated binding was observed to soluble ICAM-1 molecules nor to ICAM-1 coated onto a plate (our unpublished data), further indicating that LFA-1 on DCs is unable to bind to its ligand independently of the assay used. Any involvement of Fc receptors in the binding to ICAM-1 Fc was excluded by preincubating the cells with a Fc receptor–blocking agent that showed no effect in the bead assay (our unpublished data).

To exclude that the decreased binding to ICAM-1 on DCs was due to decreased expression levels, we detected LFA-1 expression by flow cytometry. Figure 1B shows that LFA-1 expression levels, detected with the mAb NKI-L15, remained unaltered during DC development.

The transition of LFA-1 from an inactive into an active state is known to depend on extracellular Ca^{2+} ions, and Ca^{2+} occupancy is reported by the α chain–specific mAb NKI-L16, which detects the L16 epitope (Keizer *et al.,* 1988; van Kooyk *et al.,* 1991, 1994). Recent studies more specifically showed that NKI-L16 recognizes a Ca^{2+}-bound extended conformation of the α subunit, typical of primed LFA-1 (Xie *et al.,* 2004). Therefore, we analyzed the L16 epitope expression on MOs and DCs. As shown in Figure 1B, the L16 epitope was highly expressed on MOs but was barely detectable on DCs.

It should be noted that the high expression level of the other β2 integrins on both MOs and DCs prevented us from analyzing other known activation reporter epitopes that involve the β2 subunit to monitor LFA-1 activation state.

Together, these observations indicate that major changes in LFA-1 adhesiveness occur during DC development.

Involvement of Lipid Rafts on LFA-1 Activity on MOs and DCs

The recruitment of active LFA-1 into specific cholesterol- and glycosphingolipids-enriched microdomains, known as lipid rafts, was proposed as additional mechanism to regulate integrin activity (Krauss and Altevogt, 1999; Leitinger and Hogg, 2002; Marwali *et al.,* 2003). Therefore, we investigated whether lipid rafts played a role in LFA-1 adhesiveness on MOs and DCs.

On MOs, the effect of MCD, a lipid raft–disrupting agent that extracts membrane cholesterol, was tested on the ICAM-1 bead adhesion assay (Figure 2A). MCD treatment inhibits binding for ~40%, indicating that lipid raft disruption partially affected LFA-1–binding capacity. Furthermore, we examined the codistribution of LFA-1 and the lipid raft marker GM1, a glycosphingolipid, on MOs and DCs, by Ab patching and confocal microscopy (Figure 2B). When cocapping was induced on MOs, LFA-1 completely colocalized with GM1 to the same extent as for the lipid raft–associated GPI-anchored protein CD55. By contrast, on DCs, LFA-1 is completely excluded from the lipid raft fraction.

Gradual exclusion of LFA-1 from these lipid microdomains parallels the loss of L16 epitope and binding capacity. Already after 3 d of monocyte differentiation, on the majority of the cells, LFA-1 no longer colocalized with GM1 (our unpublished data).

On MOs, we quantified the colocalization of either NKI-L15 (total LFA-1) or NKI-L16 (primed LFA-1) with GM1 by calculating the Manders coefficient (Costes *et al.,* 2004). No significant differences in colocalization with lipid rafts were observed between primed and total LFA-1 (Figure 2C), suggesting that on MO LFA-1 resides in lipid rafts even if the molecule is not in the Ca^{2+}-bound extended primed conformation. Finally, the colocalization coefficient for LFA-1 and GM1 on DCs was found to be 0.14 ± 0.24 ($n = 25$), where 1 indicate full colocalization, thus indicating a significant exclusion of LFA-1 from lipid raft domains on DCs.

LFA-1 Is Organized in Nanoclusters on MOs

The organization of the cell membrane has been described as a mosaic of numerous lipid and protein microdomains ranging from 20 to 500 nm (Mayor and Rao, 2004). The fact that

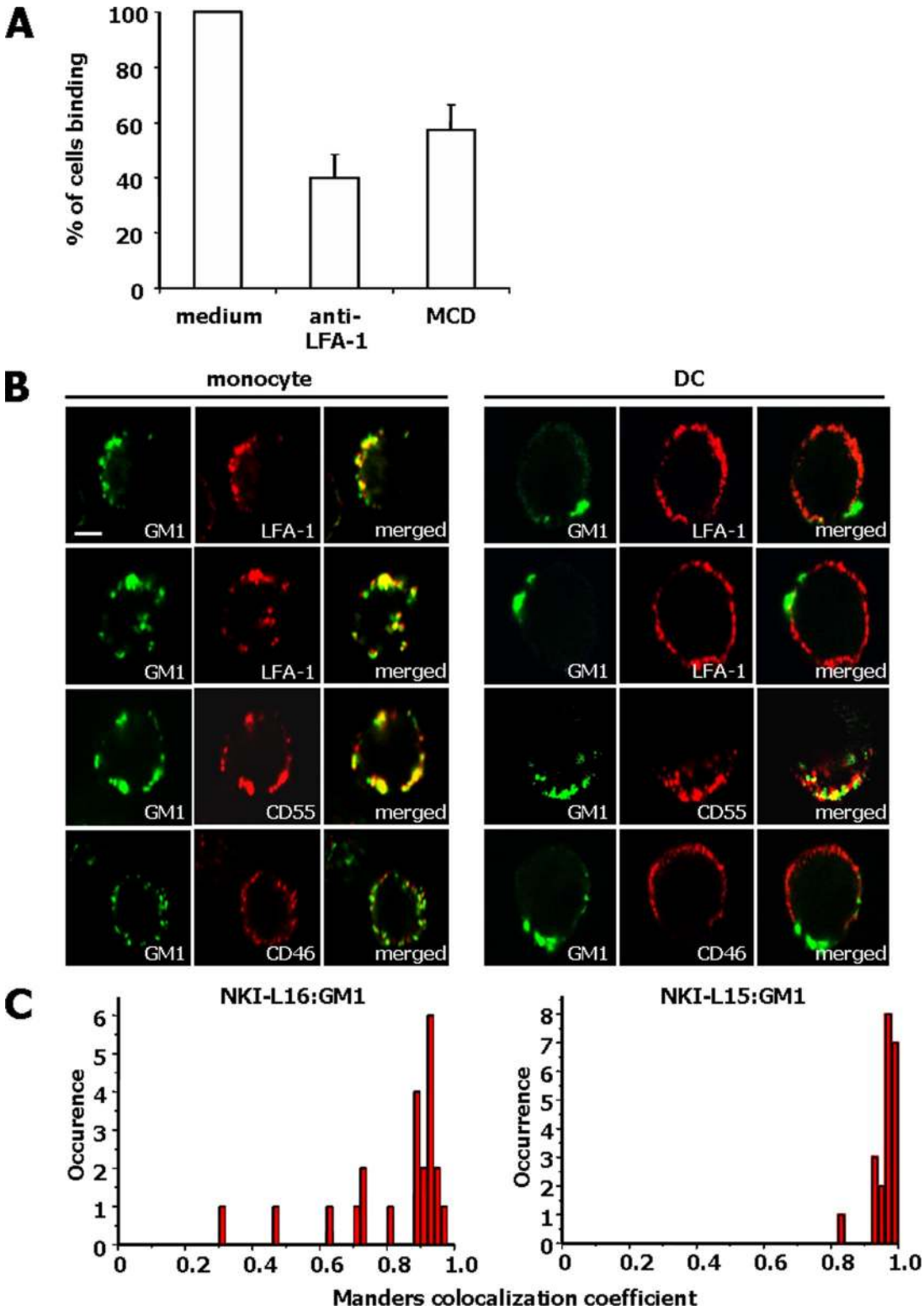

Figure 2. LFA-1 resides in lipid rafts on MOs, not on DCs. (A) LFA-1–mediated adhesion to ICAM-1–coated beads was measured on MOs after cholesterol depletion by preincubation with 20 mM MCD for 30 min at 37°C. Data shown are means ± SD of one representative experiment (out of three) performed in triplicate. (B) Confocal microscopy analysis of copatching of LFA-1 (NKI-L15 labeled) and GM1 on MOs and DCs. Receptor copatching and staining were performed as described in *Material and Methods.* CD55 and CD46 are positive and negative lipid rafts marker, respectively. Results are representatives of multiple cells in three independent experiments. Bar, 5 μm. (C) To quantify the degree of colocalization between either NKI-L15 (total LFA-1) or NKI-L16 (primed LFA-1) with GM1 on MOs, the Manders coefficient (M1) was calculated. M1 can vary between 0 and 1 (1 = colocalization). Receptor copatching and staining were performed as described in *Material and Methods,* and cells were analyzed by confocal microscopy (n = 22).

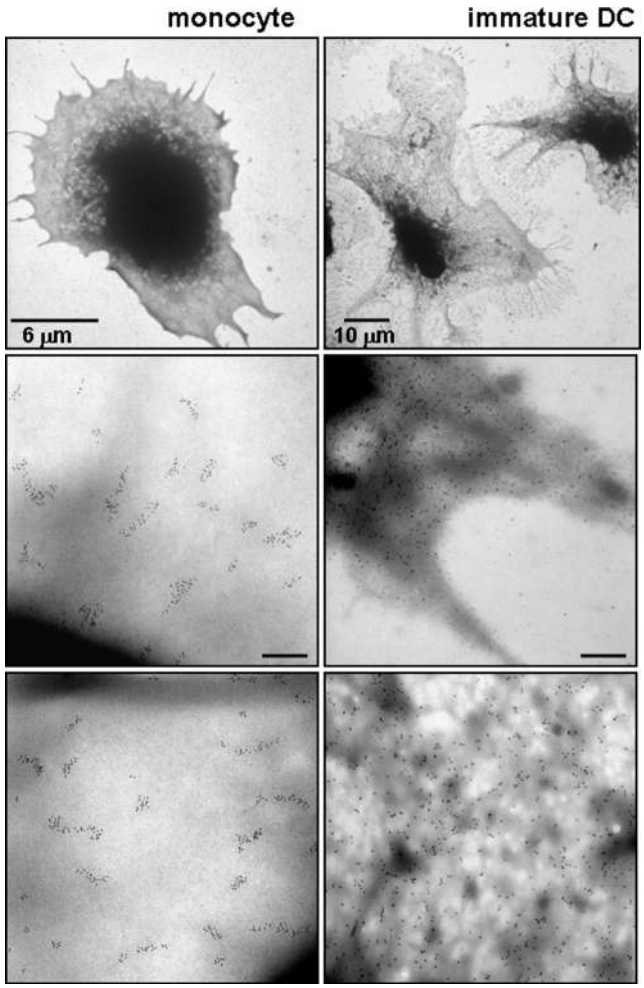

Figure 3. LFA-1 is clustered on MOs and random on DCs. MOs and DCs were specifically labeled with 10-nm gold and treated for TEM (see *Materials and Methods*). Results represent multiple cells in several independent experiments. The top pictures represent whole cells imaged by TEM. Middle and bottom pictures are higher magnifications where 10-nm gold particles are visible. Bar, 200 nm unless otherwise indicated.

LFA-1 differentially associates with lipid rafts on MOs and DCs (Figure 2) prompted us to investigate the cell membrane organization of LFA-1 at high resolution.

We exploited TEM to study whole-mount samples of MOs and DCs, after specific labeling of LFA-1 with gold particles. Recently, we and others demonstrated the potential of this method to map and quantitate the distribution patterns of cell membrane receptors (Vereb *et al.*, 2000; Panyi *et al.*, 2003; Cambi *et al.*, 2004).

MOs and DCs were allowed to adhere and stretch before labeling with mAb against LFA-1 and gold particles. It should be noted that the stretched cells are so thin (down to 200 nm at cell periphery) that sectioning is not required, thus making the whole dorsal membrane available for gold labeling and subsequent TEM analysis. To exclude any effect of the substrate on LFA-1 distribution, TEM analysis was also performed on cells that were gold-labeled in suspension and then mounted onto PLL. No differences were seen between cells stretched on the support or cells adhering to PLL (our unpublished data). We found that LFA-1 distribution changed dramatically during DC development (Figure 3). Although on MOs LFA-1 is organized in well-defined nanoclusters, on DCs the gold particles are evenly distributed over the cell surface.

To quantitatively describe LFA-1 distribution pattern, nearest neighbor (nn) distance values among the gold particles were calculated applying spatial-point-pattern analysis (Cambi *et al.*, 2004). On MOs, almost 80% of the gold particles resides within 50-nm distance from its nearest neighbor (Figure 4A). In contrast, on DCs, nn distance values are almost equally distributed in all distance categories, indicating no preferential organization of gold particles.

The relative partitioning of gold particles in clusters of various sizes (i.e., number of particles/cluster) was also quantified (Figure 4B). Although on MOs only 20% of gold particles were detected as single features, on DCs up to 70% of gold particles were found as isolated single features on the cell membrane.

LFA-1 nanoclusters appear either as round or slightly elongated features, with an indicative average diameter of 150 nm, and are randomly localized on the cell. Similarly to NKI-L15, NKI-L16 staining also showed clustered distribution of gold-labeled LFA-1 on MO cell membrane (Figure 5A). However, when LFA-1 was labeled by NKI-L16, the number of gold particles per μm^2 was approximately fourfold lower when compared with NKI-L15 labeled cells (Figure 5B). Labeling with TS2/4 mAb, which recognizes another (inert) LFA-1 epitope, gave results similar to NKI-L15 (our unpublished data).

To exclude that differences in the amount of gold particles per μm^2 were due to differences in Ab labeling efficiency, we also calculated the density of LFA-1 clusters on the cell surface (Figure 5C). NKI-L16 labeled only one third of LFA-1 clusters detectable on MO cell membrane. Again, TS2/4 labeling gave similar results when compared with NKI-L15 (our unpublished data). In addition, all mAbs showed similar distributions of nn distance values among gold particles (Figure 5D) and comparable cluster sizes (Figure 5E). This indicates that LFA-1 nanoclusters labeled by NKI-L16 are similar to the NKI-L16 negative nanoclusters in terms of density and size, but represent a primed fraction of LFA-1 that strongly binds Ca^{2+} and is in an extended (primed) conformation. MOs express LFA-1 and ICAM-1, facilitating the formation of aggregates of cells. Because it was suggested that ICAM-1 ligation might trigger LFA-1 microclusters formation (Kim *et al.*, 2004), cells were seeded at low density to avoid stimulation by homotypic aggregation and were extensively washed allowing LFA-1 distribution to equilibrate before labeling for TEM was performed. Furthermore, inhibition of LFA-1/ICAMs interactions in *cis* does not alter LFA-1 nanocluster organization (Supplementary Figure 3).

Therefore, on MO LFA-1 nanoclusters are formed in a ligand-independent manner. Although most LFA-1 nanoclusters are in a resting state, ~25% are in a primed state (L16 epitope expressed). Notably, L16 epitope expression is confined to a subset of nanoclusters rather than equally distributed over all clusters, suggesting the existence of clusters representing distinct states of integrin activation. MO differentiation into DC leads to complete dispersion of the nanoclusters and subsequent random distribution of single inactive LFA-1 molecules.

Primed LFA-1 Nanoclusters Readily Bind to ICAM-1

To further investigate the difference between primed and resting LFA-1 nanoclusters, we performed double labeling of LFA-1 using NKI-L16 and TS2/4 (nonoverlapping epitopes). As shown in Figure 6A, all LFA-1 nanoclusters are detectable by TS2/4, but only a subpopulation of these also shows expression of the L16 epitope (indicated in yellow). Interestingly, when MOs were seeded at high density,

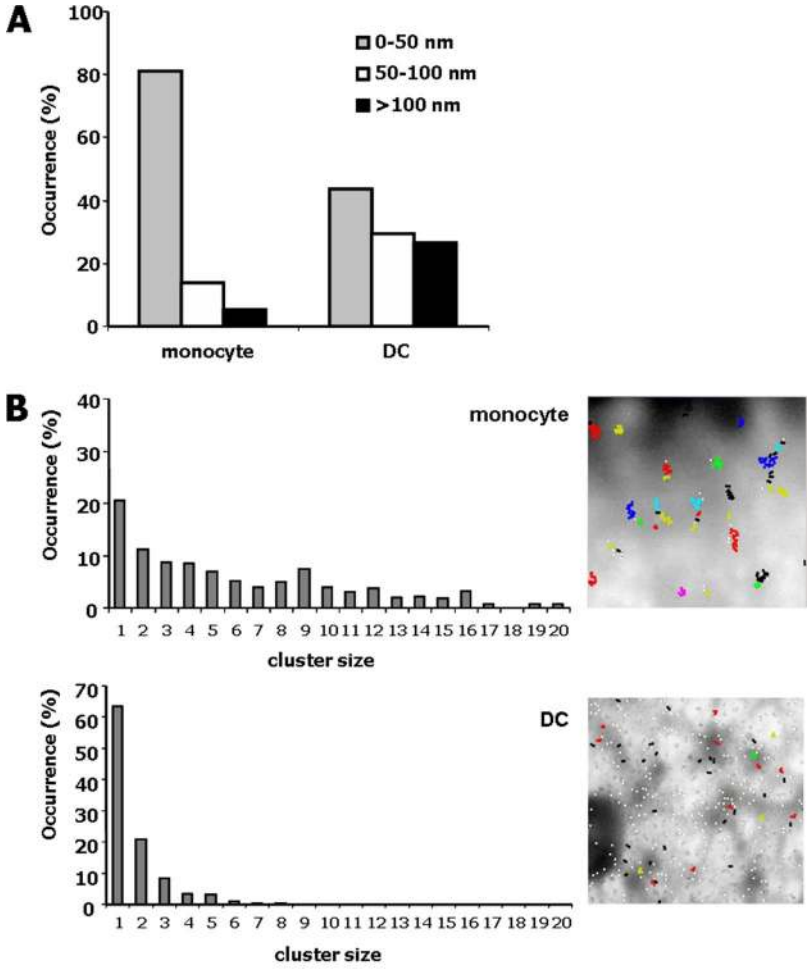

Figure 4. Quantitative analysis of the distribution of gold particles labeling LFA-1. The digital images were processed by a custom-written software based on Labview. Gold labels were counted, and coordinates were assigned to each feature. Interparticle distances were calculated using a nearest neighbor (nn) distance algorithm. (A) nn distance values were calculated for each image, and the data of several independent experiments were pooled. Subsequently, the nn distances were divided into three classes: 0–50, 50–100, and >100 nm, and the percentage of nn distance values falling into each class was plotted. (B) The partitioning of gold labels in clusters of various size (i.e., number of particles/cluster) was also quantified. Clusters were defined when gold particles were <50 nm apart from a neighboring particle. The percentage of gold particles involved in the formation of a certain cluster size was calculated. The insets are two representative processed digital images, where each type of cluster is shown in a different color. One representative experiment out of three is shown.

primed L16 epitope expressing LFA-1 was specifically enriched at the contact zone between adjacent cells, indicating that binding of ligand leads to preferential recruitment of primed LFA-1 clusters (Figure 6B).

To test if the primed LFA-1 fraction at the contact site between adjacent cells was specifically involved in the binding to ICAM-1 on the opposing cell, we allowed the formation of conjugates between individual MOs and performed triple labeling to detect total LFA-1, primed LFA-1, and ICAM-1 simultaneously. The primed LFA-1 fraction completely colocalized with ICAM-1 at the contact sites, forming macroclusters up to a size of several micrometers (Figure 6C).

Although several proteins have been identified that bind to the cytoplasmic tails of integrins (Liu *et al.*, 2000), accumulating evidence suggests that talin plays a central role in activating LFA-1 (Kupfer and Singer, 1989; Monks *et al.*, 1998; Sampath *et al.*, 1998). In verifying which cytoplasmic regulators of LFA-1 were present at the contact sites, we observed that LFA-1 macroclusters engaged in binding with ICAM-1 completely colocalize with talin, which is clearly enriched at the contact sites (Figure 6D). Although we did not find a similar enrichment of other known regulators of LFA-1 such as cytohesin-1 (Geiger *et al.*, 2000) and RapL (Katagiri *et al.*, 2003; Figure 6, E and F), we cannot exclude that these proteins may have either a transient or a weaker role in regulating LFA-1 adhesion on MOs.

Next, we investigated whether the interaction of LFA-1 with talin is essential in the formation of primed nanoclusters even in absence of ligand binding. Ligand-independent Ab-induced capping of primed LFA-1 did not result in clear colocalization of the cytoplasmic proteins talin, cytohesin, and RapL, suggesting that the expression of the L16 epitope is not the result of pre-existing ligand-independent association of the cytoplasmic tails of LFA-1 with any of its known regulators (Supplementary Figure 1).

From these results we conclude that on the cell membrane of MO LFA-1 molecules are organized in nanoclusters formed without prior engagement of ligand and independent from known intracellular regulators such as talin.

Primed LFA-1 Nanoclusters Are Dynamically Recruited at MO–T-cell Interface and Form Macroclusters

In an attempt to understand if these LFA-1 macroclusters localized at the contact site between adjacent cells were derived from the dynamic recruitment of pre-existing nanoclusters of primed LFA-1, we analyzed contact formation between MOs and T-cells in real time. Freshly isolated MOs were allowed to adhere onto glass coverslips and prelabeled with fluorescent mAb TS2/4 and with NKI-L16, which was detected by a fluorescent secondary Fab fragment. After washing unbound Abs, T-cells were added, and the formation of MO–T-cell conjugates was followed in time. It is important to note that resting T-cells express ICAM-1 but do not express the L16 epitope and do not spontaneously bind to ICAM-1, indicating that on these T-cells LFA-1 is resting (our unpublished data). In Figure 7A, a clear enrichment of

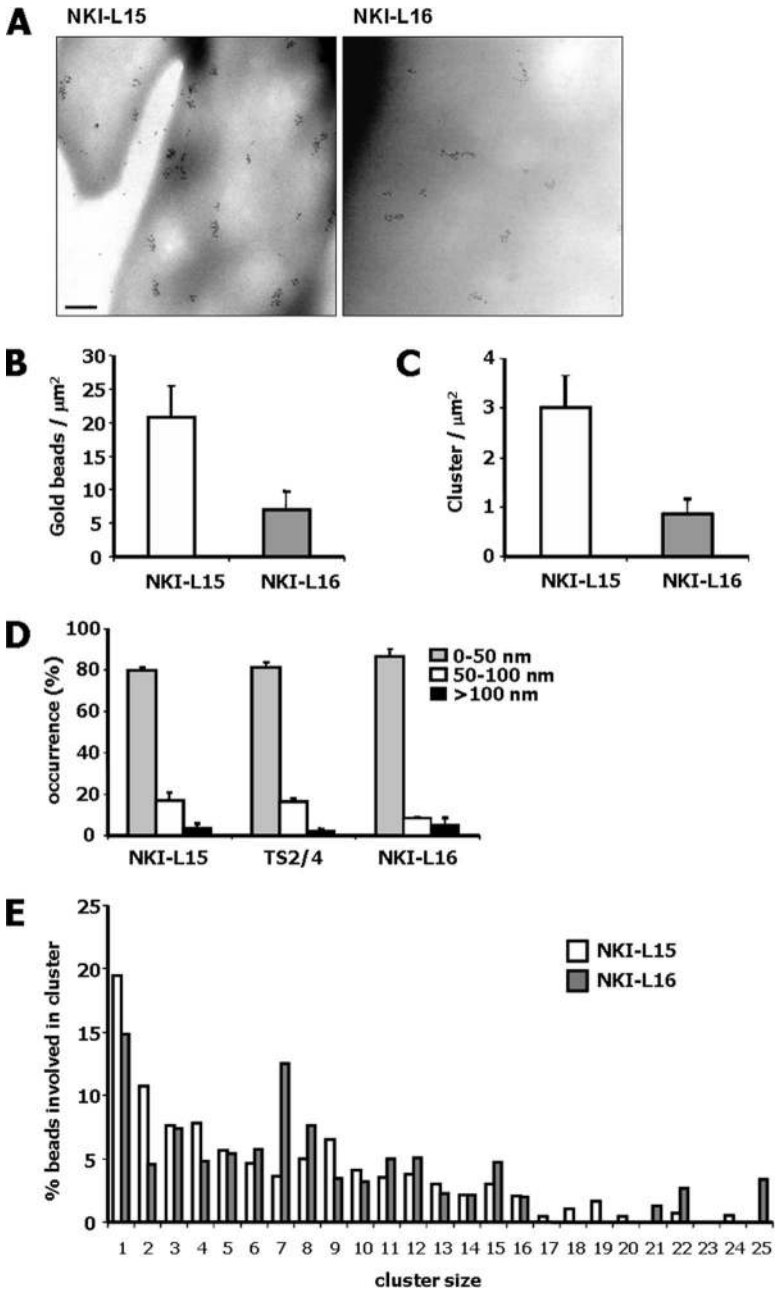

Figure 5. Resting and primed ligand-independent LFA-1 nanoclusters are expressed on the MO plasma membrane. (A) MOs were labeled as described in Figure 4, and the distribution patterns obtained with different anti-αL mAbs were compared. (B) Quantitative analysis of the distribution of gold particle labeling LFA-1 was performed as described in Figure 4B, and gold labels detected per μm^2 were counted. (C) Also, the number of clusters per μm^2 was calculated. (D) The percentage of nn distance values falling into each class was plotted. Data are the mean of three independent experiments $\pm$SD. (E) The partitioning of gold labels in clusters of various size was also quantified and compared between the mAbs. Clusters were defined as described in Figure 4B. One representative experiment out of three is shown. Scale bar, 200 nm.

primed LFA-1 molecules can be observed at the contact area between MOs and T-cells from 270 to 810 s after contact initiation. Importantly, the presence of neither TS2/4 nor NKI-L16 significantly increases binding of MOs (nor of DCs) to ICAM-1–coated beads (our unpublished data), suggesting that the cell–cell interaction cannot be attributed to the presence of these Abs. When the interaction between MOs and T-cells occurred in presence of the blocking mAb NKI-L15, hardly any conjugate was observed, and no recruitment of primed LFA-1 could be detected (Figure 7B).

Finally, we quantified the recruitment of primed LFA-1 fraction (L16 positive) with respect to the total LFA-1 (labeled by TS2/4 or NKI-L15) by calculating the recruitment index (RI), which we defined as the fluorescence intensity at the contact area divided by the fluorescence intensity of the whole cell (Figure 8). Figure 8A shows that primed LFA-1 is significantly enriched at the cell–cell contact site with respect to the total LFA-1 fluorescence signal. In presence of the blocking Ab NKI-L15, no clear interaction between MOs and T-cells could be observed, and no specific recruitment of LFA-1 was observed at the cell–cell contact (Figure 8B).

Together, these results indicate that ligand-independent primed LFA-1 nanoclusters are preformed LFA-1 platforms rapidly recruited to the cell–cell contact where they fuse to originate micrometer-sized macroclusters. The LFA-1 macroclusters are engaged in ligand binding and specifically interact with the cytoskeleton via talin.

DISCUSSION

The leukocyte specific β2 integrin LFA-1 regulates cell adhesion, migration, and immunological synapse formation. Here

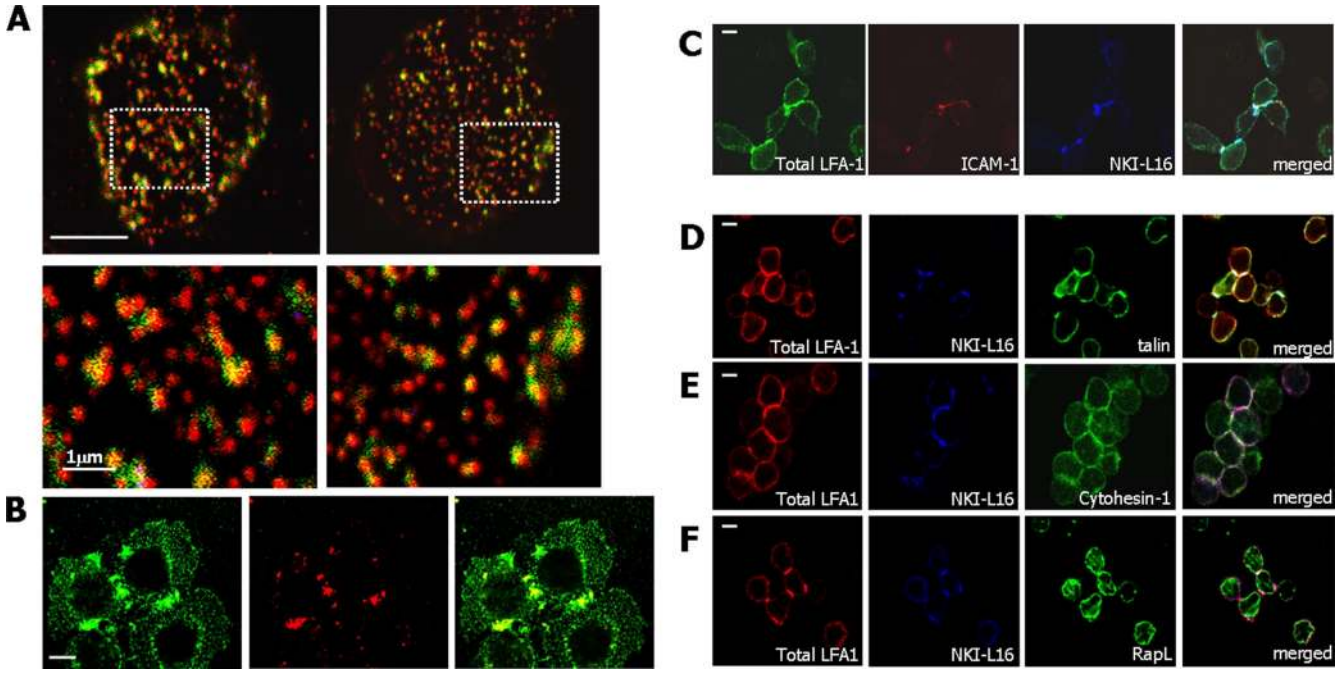

Figure 6. The primed LFA-1 molecules colocalize with ICAM-1 and talin at the cell–cell contacts. (A) MOs were allowed to adhere onto PLL-coated glass coverslips for 30 min at 37°C. After extensive washing with cold PBS, cells were incubated with TS2/4 (red) and NKI-L16 (green) on ice for 30 min to label total LFA-1 and primed LFA-1, respectively. Unbound Abs were removed, and cells were fixed with 2% PFA. Isotype specific Alexa-conjugated goat anti-mouse Abs were added. The cells were analyzed by confocal microscopy, and colocalization is indicated in yellow. (B) MOs were seeded at high density on PLL-coated glass coverslips and labeled as described for A. Total LFA-1 is shown in green and primed fraction in red. Colocalization is indicated in yellow in the merged picture. Subsequently, triple labeling for total LFA-1 (green), primed LFA-1 (blue), and various interactors (red), such as the ligand ICAM-1 (C), talin (D), cytohesin-1 (E), and RapL (F), was performed on high-density seeded MOs. Colocalization is shown in the merged pictures. Bar, 10 μm, unless otherwise indicated.

we demonstrate for the first time, exploiting high-resolution TEM and spatial-point pattern analysis, that LFA-1–mediated cell adhesion is directly correlated with submicrometer-sized avidity changes of LFA-1 when MOs differentiate into DCs.

On DC LFA-1 Is Inactive

MOs can readily differentiate into antigen-presenting DC upon reverse transmigration of endothelial monolayers (Randolph *et al.*, 1998) or when cultured in vitro in presence of GM-CSF and IL-4 (Romani *et al.*, 1996). Therefore, by using MOs and moDCs instead of LFA-1 transfectants we followed changes in the behavior of endogenous adhesion receptors in a semiphysiological system. Moreover, moDC are currently manipulated ex vivo for antitumor and antiviral therapy (Figdor *et al.*, 2004). Detailed characterization of the migratory and adhesive properties of moDCs is therefore very important and can have direct consequences for the currently executed clinical trials.

Although MOs and DCs express equivalent levels of LFA-1, there is a marked difference in LFA-1 activation state on the two cell types (Figure 1A). High-resolution mapping of LFA-1 cell surface distribution patterns by TEM and quantitative spatial point pattern analysis now revealed that on DCs the resting LFA-1 molecules are randomly distributed on the cell membrane as single features (Figure 3). Similar observations were made on K562 cells transfected with LFA-1 (K-LFA-1), which do not bind ICAM-1 and exhibit a random cell surface distribution of LFA-1 (our unpublished data). These data are in agreement with recent observation that the absence of FRET-detectable microclustering corresponds with lack of binding activity on K-LFA-1 cells (Kim *et al.*, 2004).

Crystallography, NMR, and negative stain EM showed different conformational states of integrin fragments, revealing structural rearrangements of both β and α subunits upon activation (Beglova *et al.*, 2002; Takagi *et al.*, 2002; Xiao *et al.*, 2004). In the low-affinity conformation, the headpiece of the integrin faces down toward the cell membrane; in the high-affinity conformation, the headpiece extends upward. This molecular switch occurs at the "genu" of the integrin subunits (Takagi and Springer, 2002). In particular, the α subunit leg has been shown to extend at the Ca^{2+}-dependent epitope near the thigh–genu interface (Xie *et al.*, 2004). This epitope appears only in the extended conformation and in the case of αL is specifically recognized by the conformation-sensitive mAb NKI-L16 (Keizer *et al.*, 1988; Xie *et al.*, 2004). We have shown that LFA-1–binding capacity is directly correlated to the expression of this epitope (Figure 1B). Because in the αL inactive conformation the L16 epitope is shielded from Ab recognition, the complete lack of L16 epitope on DCs suggests that all LFA-1 molecules are in the "off," i.e., bent conformation. A recent publication of van Gisbergen *et al.* (2005) suggests that on DCs inactive LFA-1 may be triggered upon interaction of DCs with T-cells (van Gisbergen *et al.*, 2005). Further studies are needed to unravel the exact signaling pathways that may trigger resting LFA-1 molecules on DCs.

LFA-1 Nanoclusters Are Either Resting or Primed

On MOs, LFA-1 is organized in primed nanoclusters (L16 positive) and resting nanoclusters (L16 negative). Because no apparent differences were found in gold particles proximity or cluster size when comparing resting and primed nanoclusters (Figure 5), we hypothesize that clustering and

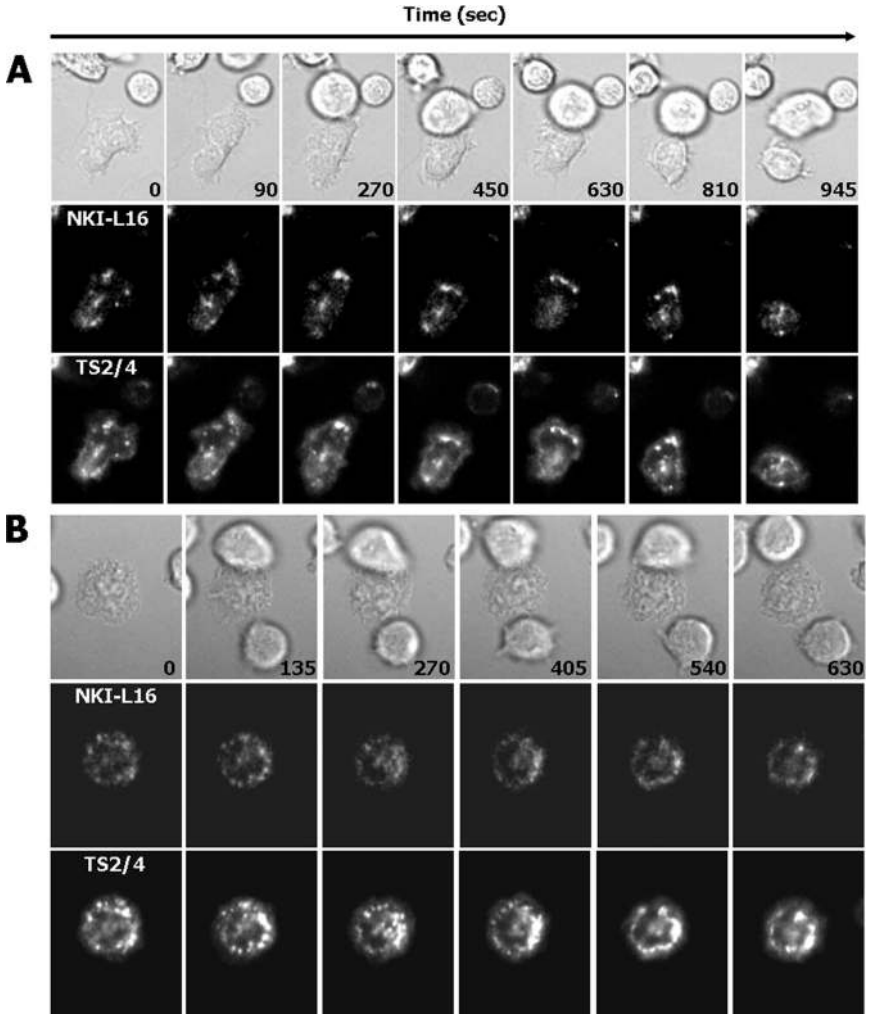

Figure 7. The primed LFA-1 nanoclusters are rapidly recruited at the MO–T-cell contact. (A) MOs were allowed to adhere at low density onto a glass coverslip for 30 min at 37°C. After washing with PBS, MOs were labeled with anti-aL mAbs NKI-L16 and TS2/4, as described in *Materials and Methods.* After removal of unbound Abs, Jurkat T-cells were added. The formation of spontaneous conjugates between MOs and T-cells was followed at 37°C with a Zeiss LSM 510 microscope. (B) In presence of the blocking mAb NKI-L15, the number of conjugates was lower, and no enrichment of NKI-L16–positive LFA-1 molecules at the cell–cell contact was observed.

priming represent two distinct events and LFA-1 molecules must all adopt either the bent inactive or the extended primed conformation within a nanocluster. The underlying mechanism remains unknown, but it is tempting to speculate that a cooperative effect between the packed LFA-1 molecules may exist. Recently, Nishiuchi *et al.* (2005) de-

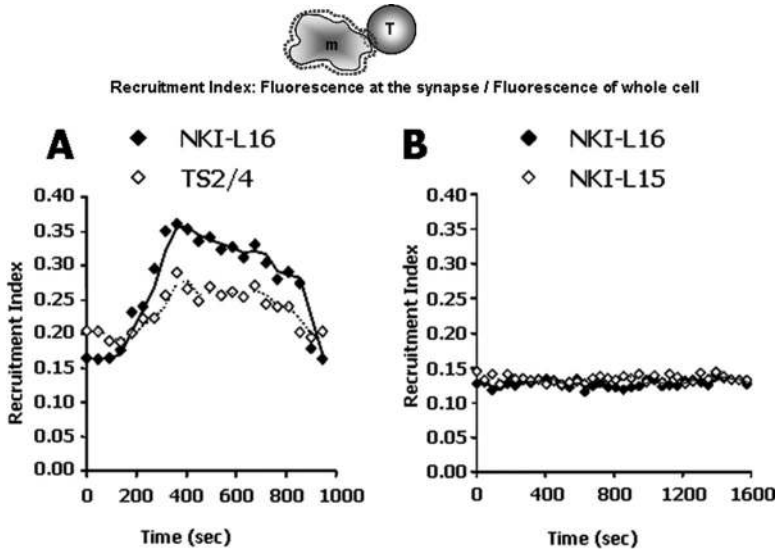

Figure 8. Quantification of the recruitment of the primed LFA-1 fraction at the MO–T-cell contact site. As shown in the cartoon, the recruitment index (RI) of each Ab was defined as the fluorescence intensity at the contact site divided by the fluorescence intensity of the whole cell. Data in A and B are referred to the images shown in Figure 7, A and B, respectively, and are representative of multiple cells in three independent experiments.

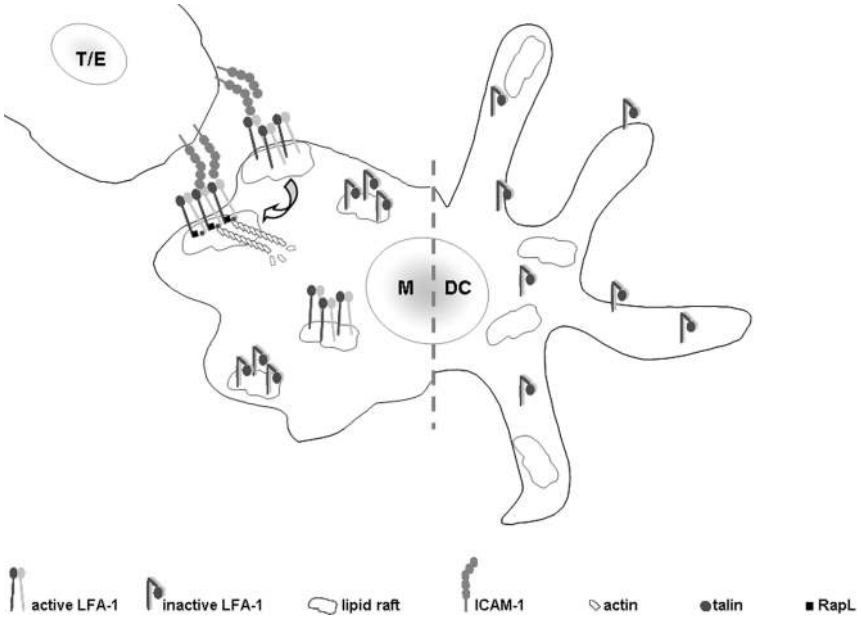

Figure 9. Major changes in LFA-1 avidity and adhesiveness occur during DC development. This cartoon summarizes the major phenotypical changes observed on DCs compared with their precursor MO. Although on immature DCs, LFA-1 is unable to bind to its ligands, is randomly distributed at the cell surface and completely excluded from the lipid rafts, on MO LFA-1 is organized in well-defined submicrometer sized nanoclusters. LFA-1 nanoclusters reside in lipid rafts but differ in terms of activation state: a fraction is primed and express the L16 epitope, the rest is in a bent resting conformation. By interaction with ICAM-1–bearing cells, the primed nanoclusters are recruited at the contact site, generating micrometer-sized macroclusters. There, LFA-1 binds to the counterreceptor ICAM-1 and establishes additional interactions with the cytoplasmic protein talin. In cell types other than MO, other regulators, such as RapL, might be then recruited from the cytoplasm and further strengthen binding and modulate signaling.

scribed the role of the tetraspanin CD151 in modulating the integrin $\alpha 3\beta 1$ adhesiveness by stabilizing its active conformation through physical interaction. Other tetraspanins were shown to be involved in the regulation of LFA-1 adhesiveness (Shibagaki *et al.*, 1999; Van Compernolle *et al.*, 2001). We are currently investigating the role of these tetraspanins in the formation of LFA-1 nanoclusters.

The arrangement of LFA-1 in nanoclusters may also guarantee an efficient binding and rebinding of LFA-1 to the ICAM-1 homodimers expressed on the endothelium. Biochemical studies showed that a divalent LFA-1 is the minimum configuration for forming efficient bonds with ICAM-1 (Sarantos *et al.*, 2005). LFA-1 nanoclusters may further increase the likelihood of LFA-1 binding to ICAM-1. Shamri *et al.* (2005) recently showed that on rolling lymphocytes LFA-1 activation occurs locally and abruptly and that priming of LFA-1 molecules (i.e., L16 epitope induction) is a prerequisite for ICAM-1–induced activation of the α subunit I-domain.

LFA-1 Nanoclusters Are Formed Independently of Ligand Binding

It has long been debated whether clustering of integrins triggers or rather results from ligand binding. Here, we present "snapshots" of the MO cell membrane, in the absence of ligand binding, where LFA-1 shows a well-defined clustered distribution pattern. Because integrin activity on circulating leukocytes is up-regulated within seconds (Shamri *et al.*, 2005), organization of LFA-1 in small predefined nanoclusters would favor instant interaction with the endothelial surface. Carman and colleagues showed that on MO linear clusters of LFA-1 colocalize with ICAM-1–containing microvilli on the endothelium before MO extravasation (Carman and Springer, 2004). Our observations extend their findings and suggest that on MO cell surface, preformed LFA-1 nanoclusters may facilitate or accelerate the interaction of MOs with these endothelial ICAM-1–enriched projections.

Although it was suggested that localized clustering of LFA-1 at the cell surface might simply result from previous encounters of LFA-1 with ICAM ligands exposed by adjacent cells (Kim *et al.*, 2004), our current findings suggest a more complex mechanism. Kim *et al.* (2004) showed that only binding of multimeric ligand (i.e., ICAM-1Fc/Anti-IgA complexes) to LFA-1–induced FRET-detectable microclustering on K-LFA-1 cells. We observed that when MOs are allowed to adhere at low density to prevent cell contact with ICAM-1 molecules from adjacent cells, nanoclusters are still present. Moreover, inhibition of LFA-1/ICAMs interactions in *cis* does not alter LFA-1 nanocluster organization (Supplementary Figure 3). Furthermore, DCs, which do not have LFA-1 nanoclusters, cannot be induced to form LFA-1 aggregates, even when cultured at high cell density (our unpublished data). However, we do not exclude that upon ligand binding a further increase in receptor packing might occur within the LFA-1 nanoclusters that would induce FRET-detectable changes in intradomain receptor proximity. Further high-resolution analysis of the integrin molecules within these assemblies is needed to provide detailed insight in the molecular and spatial organization of LFA-1 nanoclusters.

LFA-1 Macroclusters Derive from the Recruitment of Pre-existing Nanoclusters

We investigated the interaction between MOs double-labeled for LFA-1 (NKI-L16 and TS2/4) and unlabeled ICAM-1–bearing T-cells by live imaging and quantified LFA-1 accumulation at the cell–cell contact (Figures 7 and 8). The RI of primed LFA-1 molecules at the MO–T-cell contact site is significantly higher than the RI of the total LFA-1 (Figure 8). This indicates that the preformed L16-positive nanoclusters act as "primed" scaffolds of LFA-1 molecules that readily bind the ligand. These scaffolds are recruited at the contact site where larger micrometer-sized macroclusters are subsequently formed (Figure 9).

Further adhesion strengthening might result from interactions of LFA-1 cytoplasmatic tails with known β2- or αL-interacting cytoplasmic regulatory proteins. We could clearly detect a specific enrichment of talin at the cell–cell interface where LFA-1 binds to ICAM-1 (Figure 6D). Strikingly, neither interactions with cytohesin-1 nor RapL were observed (Figure 6, E and F), suggesting that the mechanism(s) regulating LFA-1 activity on MOs may differ from

those on T-cells, where both proteins were found to modulate LFA-1 function (Geiger *et al.*, 2000; Katagiri *et al.*, 2003).

Our observation that nanocluster formation does not require interaction with talin, whereas ligand-engaged macroclusters fully colocalize with talin, is in agreement with findings of Shamri *et al.* (2005). They observed that LFA-1 tethering to low-density ICAM-1 under shear flow does not require intact talin, whereas at increasing ICAM-1 density, the contribution of talin also increases (Shamri *et al.*, 2005). In addition, Xie *et al.* (2004) have mapped the L16 epitope by using a chimeric construct where extracellular α and β chains were fused to the same transmembrane anchoring domain of platelet-derived growth factor receptor. This construct allows the chimeric protein to be displayed on the cell surface but lacks the integrin cytoplasmic tail motifs that modulate the interaction with talin. Therefore, the formation of ligand-independent primed nanoclusters does not require interaction between LFA-1 and talin, whereas strengthening of cell–cell contacts is specifically supported by the presence of talin.

LFA-1 Nanoclusters and Lipid Rafts

The organization of membrane receptors in microdomains is often associated with their colocalization with lipid rafts. On T-cells, only active LFA-1 was found to reside in lipid rafts (Leitinger and Hogg, 2002). Interestingly, our studies on MOs show that both primed and resting LFA-1 nanoclusters colocalize with lipid rafts, indicating that neither clustering nor association with lipid rafts per se are sufficient for priming of LFA-1. However, on DCs random inactive LFA-1 is completely excluded by the lipid raft environment (Figure 2). The mechanism by which integrins are recruited into lipid rafts remains unclear. Because no clear lipid modification (such as myristoylation or palmitoylation) has been reported for integrin molecules, the differentiated association of LFA-1 with lipid rafts is most likely regulated by complex formation between the integrin and other as yet undefined membrane proteins.

The organization of LFA-1 in nanoclusters residing in lipid rafts may also explain why HIV-1 particles bearing host-derived ICAM-1 are efficiently spread by MOs but not by moDCs (Bounou *et al.*, 2004). Recently, we made similar observations for DC-SIGN, which binds and internalizes HIV-1 particles only when it is organized in submicrometer-sized microdomains, not when randomly distributed (Cambi *et al.*, 2004). Therefore, LFA-1 nanoclusters on MOs may be exploited by host-derived ICAM-1-bearing HIV-1 through a similar mechanism using LFA-1 nanoclusters as docking platforms.

CONCLUSIONS

We demonstrated that phenotypical changes occurring during development of precursor cells such as MOs into DCs involve also rearrangement of receptor organization at the cell surface. By using high resolution microscopy, we visualized distinct stages of integrin avidity: random inactive molecules, ligand-independent nanoclusters, and ligand-triggered macroclusters. Our findings reveal a novel mechanism to regulate integrin function. Well-defined pre-existing nanoclusters of LFA-1 equip the cell with a machinery to respond instantly when action is required, such as binding to endothelium or interacting with other leukocytes. The absence of these nanoclusters on human moDCs explains why these cells lack the capacity to bind ICAM-1 despite significant expression of LFA-1. The present challenge is to better understand the mechanism that regulates the submicrometer-sized avidity changes of LFA-1 during DC development.

ACKNOWLEDGMENTS

We thank Huib Croes for his help with the EM studies. This work was supported by Stichting voor Fundamenteel Onderzoek der Materie (FOM) to M.K. and the Dutch Cancer Society (KWF) to F.v.L. C.G.F. is supported by Grant NWO 901-10-092 from the Netherlands Organisation for Scientific Research. The authors do not have any conflicting financial interests.

REFERENCES

Banchereau, J., and Steinman, R. M. (1998). Dendritic cells and the control of immunity. Nature *392*, 245–252.

Bazzoni, G., and Hemler, M. E. (1998). Are changes in integrin affinity and conformation overemphasized? Trends Biochem. Sci. *23*, 30–34.

Beals, C. R., Edwards, A. C., Gottschalk, R. J., Kuijpers, T. W., and Staunton, D. E. (2001). CD18 activation epitopes induced by leukocyte activation. J. Immunol. *167*, 6113–6122.

Beglova, N., Blacklow, S. C., Takagi, J., and Springer, T. A. (2002). Cysteine-rich module structure reveals a fulcrum for integrin rearrangement upon activation. Nat. Struct. Biol. *9*, 282–287.

Bounou, S., Giguere, J. F., Cantin, R., Gilbert, C., Imbeault, M., Martin, G., and Tremblay, M. J. (2004). The importance of virus-associated host ICAM-1 in human immunodeficiency virus type 1 dissemination depends on the cellular context. FASEB J. *18*, 1294–1296.

Cambi, A., *et al.* (2004). Microdomains of the C-type lectin DC-SIGN are portals for virus entry into dendritic cells. J. Cell Biol. *164*, 145–155.

Carman, C. V., Jun, C. D., Salas, A., and Springer, T. A. (2003). Endothelial cells proactively form microvilli-like membrane projections upon intercellular adhesion molecule 1 engagement of leukocyte LFA-1. J. Immunol. *171*, 6135–6144.

Carman, C. V., and Springer, T. A. (2003). Integrin avidity regulation: are changes in affinity and conformation underemphasized? Curr. Opin. Cell Biol. *15*, 547–556.

Carman, C. V., and Springer, T. A. (2004). A transmigratory cup in leukocyte diapedesis both through individual vascular endothelial cells and between them. J. Cell Biol. *167*, 377–388.

Costes, S. V., Daelemans, D., Cho, E. H., Dobbin, Z., Pavlakis, G., and Lockett, S. (2004). Automatic and quantitative measurement of protein-protein colocalization in live cells. Biophys. J. *86*, 3993–4003.

de Fougerolles, A. R., and Springer, T. A. (1992). Intercellular adhesion molecule 3, a third adhesion counter-receptor for lymphocyte function-associated molecule 1 on resting lymphocytes. J. Exp. Med. *175*, 185–190.

de Fougerolles, A. R., Stacker, S. A., Schwarting, R., and Springer, T. A. (1991). Characterization of ICAM-2 and evidence for a third counter-receptor for LFA-1. J. Exp. Med. *174*, 253–267.

Dransfield, I., and Hogg, N. (1989). Regulated expression of Mg2+ binding epitope on leukocyte integrin alpha subunits. EMBO J. *8*, 3759–3765.

Dustin, M. L., and Springer, T. A. (1989). T-cell receptor cross-linking transiently stimulates adhesiveness through LFA-1. Nature *341*, 619–624.

Figdor, C. G., de Vries, I. J., Lesterhuis, W. J., and Melief, C. J. (2004). Dendritic cell immunotherapy: mapping the way. Nat. Med. *10*, 475–480.

Geiger, C., *et al.* (2000). Cytohesin-1 regulates beta-2 integrin-mediated adhesion through both ARF-GEF function and interaction with LFA-1. EMBO J. *19*, 2525–2536.

Geijtenbeek, T. B., Krooshoop, D. J., Bleijs, D. A., van Vliet, S. J., van Duijnhoven, G. C., Grabovsky, V., Alon, R., Figdor, C. G., and van Kooyk, Y. (2000a). DC-SIGN-ICAM-2 interaction mediates dendritic cell trafficking. Nat. Immunol. *1*, 353–357.

Geijtenbeek, T. B., *et al.* (2000b). DC-SIGN, a dendritic cell-specific HIV-1-binding protein that enhances trans-infection of T cells. Cell *100*, 587–597.

Geijtenbeek, T. B., Torensma, R., van Vliet, S. J., van Duijnhoven, G. C., Adema, G. J., van Kooyk, Y., and Figdor, C. G. (2000c). Identification of DC-SIGN, a novel dendritic cell-specific ICAM-3 receptor that supports primary immune responses. Cell *100*, 575–585.

Geijtenbeek, T. B., van Kooyk, Y., van Vliet, S. J., Renes, M. H., Raymakers, R. A., and Figdor, C. G. (1999). High frequency of adhesion defects in B-lineage acute lymphoblastic leukemia. Blood *94*, 754–764.

Grakoui, A., Bromley, S. K., Sumen, C., Davis, M. M., Shaw, A. S., Allen, P. M., and Dustin, M. L. (1999). The immunological synapse: a molecular machine controlling T cell activation. Science *285*, 221–227.

Katagiri, K., Maeda, A., Shimonaka, M., and Kinashi, T. (2003). RAPL, a Rap1-binding molecule that mediates Rap1-induced adhesion through spatial regulation of LFA-1. Nat. Immunol. *4*, 741–748.

Keizer, G. D., Visser, W., Vliem, M., and Figdor, C. G. (1988). A monoclonal antibody (NKI-L16) directed against a unique epitope on the alpha-chain of human leukocyte function-associated antigen 1 induces homotypic cell-cell interactions. J. Immunol. *140*, 1393–1400.

Kim, M., Carman, C. V., Yang, W., Salas, A., and Springer, T. A. (2004). The primacy of affinity over clustering in regulation of adhesiveness of the integrin áLâ2. J. Cell Biol. *167*, 1241–1253.

Krauss, K., and Altevogt, P. (1999). Integrin leukocyte function-associated antigen-1-mediated cell binding can be activated by clustering of membrane rafts. J. Biol. Chem. *274*, 36921–36927.

Kupfer, A., and Singer, S. J. (1989). The specific interaction of helper T cells and antigen-presenting B cells. IV. Membrane and cytoskeletal reorganizations in the bound T cell as a function of antigen dose. J. Exp. Med. *170*, 1697–1713.

Leitinger, B., and Hogg, N. (2002). The involvement of lipid rafts in the regulation of integrin function. J. Cell Sci. *115*, 963–972.

Liu, S., Calderwood, D. A., and Ginsberg, M. H. (2000). Integrin cytoplasmic domain-binding proteins. J. Cell Sci. *113*(Pt 20), 3563–3571.

Lu, C., Shimaoka, M., Ferzly, M., Oxvig, C., Takagi, J., and Springer, T. A. (2001a). An isolated, surface-expressed I domain of the integrin alphaLbeta2 is sufficient for strong adhesive function when locked in the open conformation with a disulfide bond. Proc. Natl. Acad. Sci. USA *98*, 2387–2392.

Lu, C., Shimaoka, M., Zang, Q., Takagi, J., and Springer, T. A. (2001b). Locking in alternate conformations of the integrin alphaLbeta2 I domain with disulfide bonds reveals functional relationships among integrin domains. Proc. Natl. Acad. Sci. USA *98*, 2393–2398.

Lub, M., van Kooyk, Y., and Figdor, C. G. (1995). Ins and outs of LFA-1. Immunol. Today *16*, 479–483.

Marlin, S. D., and Springer, T. A. (1987). Purified intercellular adhesion molecule-1 (ICAM-1) is a ligand for lymphocyte function-associated antigen 1 (LFA-1). Cell *51*, 813–819.

Martz, E. (1987). LFA-1 and other accessory molecules functioning in adhesions of T and B lymphocytes. Hum. Immunol. *18*, 3–37.

Marwali, M. R., Rey-Ladino, J., Dreolini, L., Shaw, D., and Takei, F. (2003). Membrane cholesterol regulates LFA-1 function and lipid raft heterogeneity. Blood *102*, 215–222.

Mayor, S., and Rao, M. (2004). Rafts: scale-dependent, active lipid organization at the cell surface. Traffic *5*, 231–240.

Monks, C. R., Freiberg, B. A., Kupfer, H., Sciaky, N., and Kupfer, A. (1998). Three-dimensional segregation of supramolecular activation clusters in T cells. Nature *395*, 82–86.

Nishiuchi, R., Sanzen, N., Nada, S., Sumida, Y., Wada, Y., Okada, M., Takagi, J., Hasegawa, H., and Sekiguchi, K. (2005). Potentiation of the ligand-binding activity of integrin alpha3beta1 via association with tetraspanin CD151. Proc. Natl. Acad. Sci. USA *102*, 1939–1944.

Panyi, G., *et al.* (2003). Colocalization and nonrandom distribution of Kv1.3 potassium channels and CD3 molecules in the plasma membrane of human T lymphocytes. Proc. Natl. Acad. Sci. USA *100*, 2592–2597.

Randolph, G. J., Beaulieu, S., Lebecque, S., Steinman, R. M., and Muller, W. A. (1998). Differentiation of monocytes into dendritic cells in a model of transendothelial trafficking. Science *282*, 480–483.

Romani, N., Gruner, S., Brang, D., Kampgen, E., Lenz, A., Trockenbacher, B., Konwalinka, G., Fritsch, P. O., Steinman, R. M., and Schuler, G. (1994). Proliferating dendritic cell progenitors in human blood. J. Exp. Med. *180*, 83–93.

Romani, N., Reider, D., Heuer, M., Ebner, S., Kampgen, E., Eibl, B., Niederwieser, D., and Schuler, G. (1996). Generation of mature dendritic cells from human blood. An improved method with special regard to clinical applicability. J. Immunol. Methods *196*, 137–151.

Sampath, R., Gallagher, P. J., and Pavalko, F. M. (1998). Cytoskeletal interactions with the leukocyte integrin beta2 cytoplasmic tail. Activation-dependent regulation of associations with talin and alpha-actinin. J. Biol. Chem. *273*, 33588–33594.

Sarantos, M. R., Raychaudhuri, S., Lum, A. F., Staunton, D. E., and Simon, S. I. (2005). Leukocyte function-associated antigen 1-mediated adhesion stability is dynamically regulated through affinity and valency during bond formation with intercellular adhesion molecule-1. J. Biol. Chem. *280*, 28290–28298.

Shamri, R., Grabovsky, V., Gauguet, J. M., Feigelson, S., Manevich, E., Kolanus, W., Robinson, M. K., Staunton, D. E., von Andrian, U. H., and Alon, R. (2005). Lymphocyte arrest requires instantaneous induction of an extended LFA-1 conformation mediated by endothelium-bound chemokines. Nat. Immunol. *6*, 497–506.

Shibagaki, N., Hanada, K., Yamashita, H., Shimada, S., and Hamada, H. (1999). Overexpression of CD82 on human T cells enhances LFA-1/ICAM-1-mediated cell-cell adhesion: functional association between CD82 and LFA-1 in T cell activation. Eur. J. Immunol. *29*, 4081–4091.

Shimaoka, M., *et al.* (2003). Structures of the alpha LI domain and its complex with ICAM-1 reveal a shape-shifting pathway for integrin regulation. Cell *112*, 99–111.

Springer, T. A. (1990). Adhesion receptors of the immune system. Nature *346*, 425–434.

Staunton, D. E., Dustin, M. L., and Springer, T. A. (1989). Functional cloning of ICAM-2, a cell adhesion ligand for LFA-1 homologous to ICAM-1. Nature *339*, 61–64.

Takagi, J., Petre, B. M., Walz, T., and Springer, T. A. (2002). Global conformational rearrangements in integrin extracellular domains in outside-in and inside-out signaling. Cell *110*, 599–611.

Takagi, J., and Springer, T. A. (2002). Integrin activation and structural rearrangement. Immunol. Rev. *186*, 141–163.

Van Compernolle, S. E., Levy, S., and Todd, S. C. (2001). Anti-CD81 activates LFA-1 on T cells and promotes T cell-B cell collaboration. Eur. J. Immunol. *31*, 823–831.

van Gisbergen, K. P., Paessens, L. C., Geijtenbeek, T. B., and van Kooyk, Y. (2005). Molecular mechanisms that set the stage for DC-T cell engagement. Immunol. Lett. *97*, 199–208.

van Kooyk, Y., van de Wiel-van Kemenade, P., Weder, P., Kuijpers, T. W., and Figdor, C. G. (1989). Enhancement of LFA-1-mediated cell adhesion by triggering through CD2 or CD3 on T lymphocytes. Nature *342*, 811–813.

van Kooyk, Y., van Vliet, S. J., and Figdor, C. G. (1999). The actin cytoskeleton regulates LFA-1 ligand binding through avidity rather than affinity changes. J. Biol. Chem. *274*, 26869–26877.

van Kooyk, Y., Weder, P., Heije, K., and Figdor, C. G. (1994). Extracellular Ca2+ modulates leukocyte function-associated antigen-1 cell surface distribution on T lymphocytes and consequently affects cell adhesion. J. Cell Biol. *124*, 1061–1070.

van Kooyk, Y., Weder, P., Hogervorst, F., Verhoeven, A. J., van Seventer, G., te Velde, A. A., Borst, J., Keizer, G. D., and Figdor, C. G. (1991). Activation of LFA-1 through a Ca2(+)-dependent epitope stimulates lymphocyte adhesion. J. Cell Biol. *112*, 345–354.

Vereb, G., *et al.* (2000). Cholesterol-dependent clustering of IL-2Ralpha and its colocalization with HLA and CD48 on T lymphoma cells suggest their functional association with lipid rafts. Proc. Natl. Acad. Sci. USA *97*, 6013–6018.

Vinogradova, O., Velyvis, A., Velyviene, A., Hu, B., Haas, T., Plow, E., and Qin, J. (2002). A. structural mechanism of integrin alpha(IIb)beta(3) "inside-out" activation as regulated by its cytoplasmic face. Cell *110*, 587–597.

Xiao, T., Takagi, J., Coller, B. S., Wang, J. H., and Springer, T. A. (2004). Structural basis for allostery in integrins and binding to fibrinogen-mimetic therapeutics. Nature *432*, 59–67.

Xie, C., Shimaoka, M., Xiao, T., Schwab, P., Klickstein, L. B., and Springer, T. A. (2004). The integrin alpha-subunit leg extends at a Ca2+-dependent epitope in the thigh/genu interface upon activation. Proc. Natl. Acad. Sci. USA *101*, 15422–15427.